

UNIVERSITY OF STOCKHOLM
INSTITUTE OF PHYSICS

REPORT

ONE, TWO AND THREE PION PRODUCTION
IN p-p COLLISIONS AT 19 GeV/c

V. Bakken, J. D. Hansen, T. Jacobsen,
H. Johansson, P. Lundborg, R. Möllerud,
J. E. Olsson, J. Mäkelä, H. Pimiä, B. Selldén
and E. Sundell

USIP Report 76 - 13

April 1976

USIP Report *76-13*

Får ej sändas till referat-
tidskrift.

ONE, TWO AND THREE PION PRODUCTION
IN pd COLLISIONS AT 19 GeV/c

V. Bakken, J. D. Hansen, T. Jacobsen,
H. Johansson, P. Lundborg, R. Möllerud,
J. E. Olsson, J. Mäkelä, H. Pimiä, B. Sellden
and E. Sundell

USIP Report 76 - 13

April 1976

ONE, TWO AND THREE PION PRODUCTION IN pd COLLISIONS AT 19 GeV/c

The Scandinavian Bubble Chamber Collaboration

V. Bakken^{*}, J.D. Hansen^o, T. Jacobsen^{*},
H. Johansson^{**}, P. Lundborg^{**}, R. Möllerud^o, J.E. Olsson^{*},
J. Mäkelä^x, H. Pimiä^x, B. Selldén^{**}, E. Sundell^{*}

ABSTRACT

We present cross sections for coherent and non-coherent production of one, two and three pions in pd reactions at 19 GeV/c. The mass distributions of the two pion non-coherent channels are studied. Strong single $\Delta(1236)$ and also some double Δ production are observed. Clear evidence for ρ production is seen.

- o) The Niels Bohr Institute, University of Copenhagen
- x) Department of Nuclear Physics, University of Helsinki
- +) Department of Physics, Åbo Akademi
- *) Institute of Physics, University of Oslo
- **) Institute of Physics, University of Stockholm

1. INTRODUCTION

In this paper we present some results from a bubble chamber study of one, two and three pion production in pd reactions at 19 GeV/c, obtained from 3-prong and 4-prong topologies. This investigation represents an extension to pn and coherent pd reactions of our earlier studies of pp reactions at 19 GeV/c [1].

Some results based on parts of the sample have been published earlier [2].

The combination of pp and pn data at the same energy offers many advantages and new possibilities, e.g. a sufficient number of charge channels are available to isolate the isospin content of the amplitudes for single pion production [2a].

The plan of the paper is the following: Section 2 contains the details of the experimental procedure; the data processing, the treatment of ambiguities and the isolation of data on free nucleon scattering. In section 3 we evaluate the channel cross sections, the corrections applied to obtain free pn cross sections and a discussion of the energy dependence of the various cross sections. In section 4 some general features of two pion production are presented.

2. EXPERIMENTAL PROCEDURE

2.1 Data processing

The data presented in this paper are based on a 200 000 pictures exposure of the CERN 2 m bubble chamber filled with deuterium to a proton beam of momentum 19.1 GeV/c. The film has been scanned for all three-prong events and for four-prong events with a spectator candidate, i.e. a heavily ionizing track stopping in the chamber with a projected length less than 22 cm. In part of the sample we have scanned and processed the full 4-prong topology. The film was double scanned with a combined scanning efficiency close to 100 %. The events recorded (50 000 events) were measured on the Danish-Swedish Spiral Reader [3] and processed through the filtering programme POOH and the standard CERN THRESH-GRIND-SLICE chain of programmes.

80 % of the recorded events were successfully measured and processed through the programme chain.

The events have been fitted to the following channels:

$$pd \rightarrow p p p \pi^- \quad (1)$$

$$pd \rightarrow p p p \pi^- \pi^0 \quad (2)$$

$$pd \rightarrow p p n \pi^+ \pi^- \quad (3)$$

$$pd \rightarrow p d \pi^+ \pi^- \quad (4)$$

$$pd \rightarrow p d \pi^+ \pi^- \pi^0 \quad (5)$$

$$pd \rightarrow n d \pi^+ \pi^+ \pi^- \quad (6)$$

In GRIND the unobserved positive track is treated in the standard way, i.e. an unobserved proton track is in the fit assigned starting momentum components

$$p_x = p_y = p_z / 1.37 = (0 \pm 30) \text{ MeV}/c$$

and with twice these errors for an undetected deuteron recoil. This procedure is reasonable for a spectatorlike particle as the undetected proton is likely to be. Also for a deuteron recoil the procedure is found to be an acceptable way of dealing with a particle having too low momentum to be detected in the chamber [4], see also section 2.2.

Reactions (1) and (4) correspond to four constraints fits for 4-prong events and pseudo-4C fits for 3-prong events. The other reactions are likewise fitted as 1C and pseudo-1C fits. Multineutral hypotheses (0-constraint fits) have not been tried.

In the kinematic programme we have applied a χ^2 -probability cut-off of 0.1 % and 1 % for the 4C and 1C hypotheses respectively. Of the kinematically acceptable hypotheses only those consistent with the observed track bubble densities were retained. We also required the fitted momentum of the faked positive track to be consistent with not being observed. In addition, the following criteria were applied to all hypotheses in order to reduce the number of false fits:

- i) There should be one baryon in the forward hemisphere and two (or a deuteron) in the backward hemisphere in the center of mass (CM) system.
- ii) The laboratory momentum of π^+ and π^0 mesons should be less than 12 GeV/c. The momentum of π^0 mesons should be less than 12 GeV/c also in the beam rest frame.
- iii) The laboratory momentum of a deuteron should be less than 500 MeV/c.

- iv) A four-constraints hypothesis is accepted over a one-constraint hypothesis except when there is a competition between a 4C coherent hypothesis and the corresponding non-coherent hypothesis.

Criteria (i) and (ii) are justified by observations in our pp-reactions at 19 GeV/c [1] and in other experiments at comparable energies. Criterium (iii) is applied to remove false fits with a high-momentum final state deuteron. Due to the deuteron form factor such reactions are very unlikely for deuteron recoil momenta above 500 MeV/c which corresponds to a four-momentum transfer squared to the deuteron of around 0.25 (GeV/c)^2 . From fig. 2, which shows the distribution of $t' = |t - t_{\min}|$ to the deuteron of reaction (4), it can be seen that criterium (iii) hardly excludes any fits to coherent reactions.

The preference of a 4C hypothesis over a 1C hypothesis is considered to be a standard procedure, but its reliability is reduced in the case of an undetected charged track (pseudo-4C fits). Because of the small binding energy of the deuteron there will at high energies practically always be a good fit to a non-coherent hypothesis if the corresponding coherent hypothesis is acceptable. In this case the preference of 4C hypotheses is questionable, in particular for the pseudo-4C fits.

2.2 Treatment of ambiguities

The procedure described above resulted in a total of 18000 accepted hypotheses corresponding to 12000 events. We have excluded from the sample, events with a fitted momentum of the slowest proton above 350 MeV/c in accordance with the range cut used at the scanning stage. 75% of the events fitted on hypothesis uniquely while 23% and 2% of the events had 2 and 3 acceptable hypotheses respectively, "internal ambiguities" included. The term "internal ambiguity", as opposed to "channel ambiguity", refers to interpretations corresponding to the same final state. The internal ambiguities, which represent ~30% of all ambiguities, do not affect the calculation of channel cross sections.

The ambiguities are of essentially two types; the first type occurs between a coherent channel and the corresponding non-coherent one because of the low deuteron binding energy, and the second type arises from a competition between a

proton and a pion mass assignment of one or a pair of positive tracks leading to either a "channel ambiguity" or an "internal ambiguity".

2.2.1 Coherent, non-coherent separation

For non-coherent reactions, e.g. $pd \rightarrow ppn\pi^+\pi^-$ there should be neither a correlation between the direction of a slow proton and a slow neutron nor a sharp enhancement in the $M(pn)$ mass distribution near the deuteron mass. If on the other hand a truly coherent reaction gives a fit to the corresponding non-coherent hypothesis the proton and the neutron are expected to be predominantly co-linear and the mass distribution $M(pn)$ for such hypotheses should show a peak at the deuteron mass. In addition one expects from range-momentum relations of the proton and the deuteron that the ratio $R = p_{\text{lab}}(ps) / p_{\text{lab}}(n)$ should be about 1.5 [4].

In fig. 1a-c we have plotted the distributions of $M(p_s n)$, $\cos\theta_{\text{lab}}(p_s n)$ and $R = p_{\text{lab}}(p_s) / p_{\text{lab}}(n)$ for 4-prong events fitting the reaction $pd \rightarrow ppn\pi^+\pi^-$. The shaded regions correspond to those events which also have an acceptable fit to the coherent reaction $pd \rightarrow pd\pi^+\pi^-$. As can be seen, the clear enhancements around the values indicated above consist almost exclusively of events with a possible coherent interpretation. The events with no acceptable coherent hypothesis exhibit a flat angular behaviour (fig. 1b), also in the region of the coherent peak. We conclude that the great majority of the 4-prong events, having both a coherent and a non-coherent interpretation, are really coherent reactions.

The $M(p_s n)$ mass distribution for the 3-prong sample, fig. 1d, shows a similar peak which is somewhat broader as expected. From a study of these and other distributions we find it reasonable to keep only the coherent hypothesis for those 4-prong events for which $M(p_s n) < 1.887$ GeV. We use the same cut for the 3-prong events but we keep both the coherent and the non-coherent hypothesis with their original weights. For both 3-prong and 4-prong events we reject the coherent hypothesis if $M(p_s n) > 1.887$ GeV.

We have some (36%) ambiguities between the channel $pd \rightarrow pd\pi^+\pi^-$ and the channel $pd \rightarrow ppn\pi^+\pi^-$. The effective mass distribution $M(p_s n)$ has a similar shape as the one of the AC 3-prong coherent channel but is somewhat broader and slightly shifted towards higher masses. In analogy with the procedure described above we accept as coherent those ambiguous events for which $M(p_s n) < 1.916$ GeV both in the 3-prong

and in the 4-prong sample. We are aware of the fact that the procedure is less reliable in this case but since the π^0 is slow in the laboratory frame for the ambiguous events, we still think it makes sense to use it.

There are no ambiguities between the channel $pd \rightarrow nd \pi^+ \pi^-$ and the non-coherent 1C channels.

The validity of our procedure to obtain a reliable coherent sample may be judged from the distribution of $t' = |t - t_{\min}|$ to the final state deuteron shown in fig. 2 for the $pd \pi^+ \pi^-$ channel. The 3-prong events are indicated by the shaded region. The combined sample exhibits an exponential behaviour down to $t' = 0$ as expected for diffractively produced events. The results of fits to an exponential $Ae^{-Bt'}$ are given in table 1. The fit to the 4-prong sample only gives a slightly higher slope but the values are consistent with being equal within errors. These values of the slope parameter are in good agreement with results at other energies [5].

We have also fitted the t' distributions for the 4-prong events of the 1C coherent channels. The results are given in table 1 and figs. 3-4. We use only the 4-prong sample since we consider the 3-prong sample unreliable.

2.2.2 The p/π^+ ambiguity

The ambiguity between a proton and a π^+ assignment to a track is most serious between the $ppp \pi^0$ and the $ppn \pi^+ \pi^-$ channels and as internal ambiguities in the $ppn \pi^+ \pi^-$ channel. The events in the π^0 -channel have an ambiguity rate of 48%. The external and internal ambiguity rates of the neutron channel are 12% and 7% respectively.

We find it justified to classify these events by selecting the hypothesis for which the difference between the longitudinal momenta of the nucleons in the center of mass frame is largest. The motivation for this choice is the well known fact that the nucleons are very peripheral in high energy NN reactions. The same method has been used in other pp and pd experiments [6, 7].

In addition we observe that the longitudinal momentum distribution of the π^+ in the center of mass frame becomes more symmetric and agrees with the one of the ambiguous events and with the one of the π^- . We estimate this test to favour the wrong hypothesis in less than 10% of the cases. The peripherality test is also used

to resolve ambiguities between the 1C coherent channels (30 %) and internal ambiguities of the $pd \pi^+ \pi^- \pi^0$ channel although these are rather few (6 %).

3. EXTRACTION OF CROSS SECTIONS

The spectator model implies that the non-coherent channels (1)-(3) correspond to interactions between the beam proton and one of the nucleons of the deuteron. The following free nucleon processes may then be studied:

$$pn \rightarrow pp \pi^- \quad (1a)$$

$$pn \rightarrow pp \pi^- \pi^0 \quad (2a)$$

$$pn \rightarrow pn \pi^+ \pi^- \quad (3a)$$

$$pp \rightarrow pp \pi^+ \pi^- \quad (3b)$$

Motivated by the impulse approximation and the fact that the Fermi momentum of the nucleons is relatively small, we define the spectator as the one of the two slow final state nucleons that has the smallest momentum in the laboratory frame. The separation of channels (3a) and (3b) thus corresponds to the labeling of different nucleons as the spectator.

According to the spectator model and the impulse approximation the observed momentum and angular distributions of the spectator should agree with what we expect from the deuteron wave function. The angular distribution of the spectator in the $pp\pi^-$ -channel is shown in fig. 5 and the line is the prediction of the model taking the invariant flux factor into account. The corresponding momentum distribution was given in ref. [2a]. In both cases the agreement is acceptable [2a].

The spectator momentum distributions for the neutron and π^0 channels are not consistent with the Hulthén distribution for unmeasured spectators. The reason for this is that there are two undetected particles in the final state and the neutral particle then absorbs the missing momentum almost completely.

The problem of separating the proton spectator and the neutron spectator channels is illustrated by the scatterplot in fig. 6a which shows the momentum of the slow proton versus the momentum of the slow neutron. The diagonal, where the two momenta are equal, represents the separation between the two channels. There is

no clear separation between them for the 4-prong sample, in particular when one recalls that in these events there is always a high-momentum track which gives a large uncertainty to the neutron momentum. In spite of this difficulty our selection procedure results in a cross section for the reaction (3b) which is consistent with the one observed with hydrogen target [16]. In this comparison we have only used that part of the sample where all 4-prong events were analyzed.

To obtain free neutron cross sections from the deuteron cross sections we have to correct for Glauber screening and for the effect of the Pauli principle. These two corrections were discussed in detail in our earlier paper [2a]. A correction of 5% for the Glauber screening has been applied to the cross sections of all non-coherent channels. The effect of the Pauli principle has been corrected for only in the $pp\pi^-$ channel since it is likely to be negligible for the other channels because of resonance production.

We then obtain the cross sections for the non-coherent channels that are given in table 2. In fig. 7 we compare our cross sections with those at other energies [5, 7, 8, 13]. The published cross section at 28 GeV for the reaction $pd \rightarrow pd\pi^+\pi^-$ is only for $M(p\pi^+\pi^-) < 2$ GeV. If we correct for this cut, using the ratio of $M(p\pi^+\pi^-) < \text{GeV}$ /all extrapolated from values of this ratio at lower energies, we get the cross section in the figure.

To calculate the cross sections for the coherent channels we use only the 4-prong events and we correct for the 3-prong events by extrapolating the t' distributions of the deuterons to $t' = 0$. If we in the 4C coherent channel base the calculation on both the 3-prong and the 4-prong events a cross section that is 5% smaller is obtained. In this channel we observe a prominent d^{*0} signal at 2.20 GeV in the $M(d\pi^-)$ distribution. In the coherent π^0 channel an even bigger d^{*+} signal is observed. If we subtract the d^* cross sections we obtain cross sections that are also given in table 2. We note that the d^{*+} signal may partly be caused by influx. The d^* phenomenon will be studied in a separate paper.

We have not undertaken any detailed study of the influx of events with an extra π^0 in the various channels. To reduce the influx we apply a probability cut of 2% in the 4C channels and of 10% in the 1C channels, which we have found results in acceptable missing mass distributions. The probability distributions are found to be flat above the cut in all channels but the 1C 3-prong coherent channels.

From the missing mass distributions for the 4C channels we estimate that the influx from events with an extra π^0 is small. The influx is difficult to estimate for the other channels. To account for systematic effects we have thus added extra errors of 3% and 10% for influx(/outflux) in the 4C and 1C channels respectively, of 10% of the ambiguous events for failures of the peripherality test in the 1C channels and of 5% and 10% of the ambiguous events for events wrongly classified as non-coherent in 4C and 1C coherent channels respectively. All errors are added quadratically.

4. RESONANCE PRODUCTION IN THE $pn \rightarrow pn\pi^+\pi^-$ AND $pn \rightarrow pp\pi^-\pi^0$ CHANNELS

We will not give any detailed analysis of these channels in this report but rather limit ourselves to the presentation of some effective mass distributions. Cross sections for some of the resonances seen in these distributions have been extracted, and will be given together with a few characteristics of the production mechanism.

The nucleons are in these reactions peripherally produced and thus we can split the neutron channel into two subchannels

$$pn \rightarrow p_F n_B \pi^+ \pi^- \quad (a)$$

$$pn \rightarrow n_F p_B \pi^+ \pi^- \quad (b)$$

where F and B denote forward and backward in the CM system. The two subchannels which correspond to 78% and 22% respectively, are completely different and show very few common characteristics.

In table 3 the longitudinal momenta of the pions has been used to identify the events with different peripheral diagrams.

4.1 $N\pi$ mass distributions

The $p_F n_B \pi^+ \pi^-$ channel is in many respects similar to the reaction $pp \rightarrow pp\pi^+\pi^-$ [1] and that is especially the case for the $p\pi^+$ effective mass distribution where large Δ^{++} (1236) signal can be seen, fig. 8 a. But in this channel we also observe an equally large Δ^- (1236) peak in the $n\pi^-$ mass distribution, fig. 8 a. It is interesting to note that while the cross section for the reaction $pp \rightarrow pp\pi^+\pi^-$ is 1.6 mb the cross section for the reaction $pn \rightarrow p_F n_B \pi^+ \pi^-$ is 2.2 mb and that the difference is almost equal to

the Δ^- cross section, table 4. To investigate any $\Delta^+ \Delta^-$ production we made a scatter plot of $M(p \pi^+)$ vs $M(n \pi^-)$, and, as can be seen in fig. 9, a clear $\Delta \Delta$ production signal is seen. Another indication of $\Delta \Delta$ production can be seen in fig. 8 a where the shaded areas show the events that have the pions in opposite hemispheres.

To extract cross sections for the Δ production we have fitted an incoherent sum of a slightly modified Breit-Wigner term of the Jackson type [9, 12c] and a peripheral background term to the mass distributions in fig. 8 a. In the $\Delta \Delta$ case the background was obtained by adding incoherently the extrapolated number of events in the $\Delta(1236)$ mass region (1.15-1.32) GeV from the two Δ -bands separately. The excess of events corrected for the tails are defined as $\Delta \Delta$ events, and the cross section is given in table 4. The associated $\Delta \Delta$ production is included in the cross sections for reactions (1) and (2).

The cross sections for associated $\Delta \Delta$ production at various energies in pn, pp and $\bar{p} \bar{p}$ reactions have been plotted in fig. 10 [7, 10, 11, 12]. From isospin invariance and dominance of isovector exchange one expects $\sigma(pn \rightarrow \Delta^{++} \Delta^-) = \sigma(\bar{p} \bar{p} \rightarrow \bar{\Delta}^{--} \bar{\Delta}^{++}) = (9/2) \sigma(pp \rightarrow \Delta^{++} \Delta^0)$. The line shown is of the form p_{lab}^{-n} with $n = 2.5$.

We have fitted double exponentials $Ae^{-b_1 t'} + Be^{-b_2 t'}$ to the t' distributions of the reactions (1)-(2) and a single exponential for reaction (3). The values are given in table 4. The variable t' is defined as $t' = |t - t_{min}|$ and the interval used in the fit is (0.00-0.46) (GeV/c)² for Δ^{++} and (0.02-0.46) (GeV/c)² for Δ^- . In case of reaction (3) there is a considerable background from single Δ production. For comparison we mention that $b_1 = 12.6 \pm 1.4$ (GeV/c)⁻² is reported for reaction (3) at 11.6 GeV/c [7].

The remaining two mass distributions i.e. $M(p_F \pi^-)$ and $M(n_B \pi^+)$ are also given in fig. 8 b. No striking structures can be seen.

For the $n_F p_B \pi^+ \pi^-$ channel the various $N\pi$ mass distributions have been plotted in fig. 12. The $n_F \pi^+$ and $p_B \pi^-$ mass distributions are dominated by broad low mass enhancements. Some production of $\Delta(1236)$ can however be seen in all the four distributions.

The scatterplot of $M(p \pi^+)$ versus $M(n \pi^-)$ shows no signal of associated $\Delta \Delta$ production. Such production would indicate the presence of exotic $\Delta Q = 2$ exchange. The cross section for this process drops rapidly with increasing energy [7] and its absence is in agreement with that observation.

The effective mass distribution of the $p\pi$ combinations in the π^0 channel are given in fig. 13. The $p_B\pi^-$ distribution is dominated by a broad low mass enhancement similar to the corresponding one in the n_F channel. Production of $\Delta(1236)$ can be seen in the two $p\pi^0$ combinations.

4.2 $N\pi\pi$ mass distributions

The various $N\pi\pi$ mass distributions are shown in figs. 13-16. The shaded regions show the distribution when the smallest $N\pi\pi$ mass combination is chosen. In the $p_F\pi^+\pi^-$ mass distribution we see a broad low mass enhancement that probably contains the $N^*(1470)$ and the $N^*(1700)$. The distribution is similar to the corresponding one of the $pp \rightarrow pp\pi^+\pi^-$ channel [1a]. The $n_B\pi^+\pi^-$ mass distribution is similar to the $p_F\pi^+\pi^-$ one as expected from the symmetry of the two systems. We have added the two distributions in fig. 14 where the smallest mass combination is chosen in each event.

The mass distribution of the $p_B\pi^-\pi^0$ system, which could be diffractively produced, peaks at lower masses, like the $p_F\pi^+\pi^-$ system.

4.3 $\pi\pi$ mass distributions

The $\pi\pi$ mass distribution for the channels $pn \rightarrow pn\pi^+\pi^-$ and $pn \rightarrow pp\pi^-\pi^0$ is shown in fig. 17. A significant peak in the ρ region is seen. The production of the ρ meson is analysed in detail in an earlier paper [2b] where also cross sections for ρ and f^0 production are given.

ACKNOWLEDGEMENTS

We wish to thank the staffs of the CERN Proton Synchrotron, of the 2m hydrogen bubble chamber and of the U5 beam for their efforts during the exposures for this experiment.

Our thanks are also due to the scanning and measuring staffs at our four universities and the staffs of the computing centers in Copenhagen, Helsinki, Oslo and Stockholm.

Supports from Research Councils in Denmark, Finland, Norway and Sweden are gratefully acknowledged.

REFERENCES

1. a) H. Johnstad, R. Møllerud, L. Veje, S. Ljung, H.I. Miettinen, R.O. Raitio, J.K. Tuominiemi, T. Jacobsen, S.O. Sørensen, L. Granström, S.O. Holmgren, U. Svedin, N. Yamdagni, Nucl. Phys. B42 (1972) 558.
- b) H. Bøggild, E. Dahl-Jensen, K.H. Hansen, H. Johnstad, E. Lohse, M. Suk, L. Veje, V.J. Karimäki, K.V. Laurikainen, E. Riipinen, T. Jacobsen, S.O. Sørensen, J. Allan, G. Blomqvist, O. Danielsson, G. Ekspong, L. Granström, S.O. Holmgren, S. Nilsson, B.E. Ronne, U. Svedin, N.K. Yamdagni, Nucl. Phys. B27 (1971) 285.
2. a) E. Dahl-Jensen, I. Dahl-Jensen, J.D. Hansen, R. Møllerud, J. Mäkelä, M. Pimiä, E. Sundell, V. Bakken, J. Haldorsen, T. Jacobsen, G. Skjeving, G. Ekspong, H. Johansson, P. Lundborg and B. Selldén, Nucl. Phys. B87 (1975) 426.
- b) V. Bakken, J.D. Hansen, T. Jacobsen, H. Johansson, P. Lundborg, J. Mäkelä, R. Møllerud, J.E. Olsson, M. Pimiä, B. Selldén and E. Sundell, Isospin analysis of single ρ and f^0 production in pN collisions at 19 GeV/c, contribution to the Conference on High Energy Physics, Palermo, 1975.
3. Proceedings of the European Spiral Reader Symposium, Stockholm, CERN 72-46 (1972).
4. P. Fleuri, Methods of Subnuclear Physics, Vol. II. (Gordon and Breach, New York, 1968) p. 560.
5. U. Karshon, G. Yekutieli, D. Yaffe, A. Shapira, E.E. Ronat and Y. Eisenberg, Nucl. Phys. B37 (1972) 371.
- H. Braun, O. Brick, A. Fridman, J.-P. Gerber, P. Juillot, G. Maurer, G. Alexander, S. Nagan, J. Grunhaus, A. Levy, D. Lissauer and Y. Oren. Coherent production features in dp interactions at 11.9 GeV/c, Contribution to the Conference on High Energy Physics, Palermo, 1975.
- J.W. Chapman, J.W. Cooper, B.P. Roe, D. Sinclair, and J.C. Van der Velde, Phys. Rev. Lett. 30 (1973) 64.
- D. Hochman, Y. Eisenberg, U. Karshon, A. Shapira, E.E. Ronat, D. Yaffe, and G. Yekutieli, Nucl. Phys. B68 (1974) 301.
6. G. Alexander, Z. Carmel, Y. Eisenberg, E.E. Ronat, A. Shapira, G. Yekutieli, A. Fridman, G. Maurer, J. Oudet, C. Zech, P. Cüer, Phys. Rev. B173 (1968) 1322.

7. D. Hochman, Y. Eisenberg, U. Karshon, A. Shapira, E. E. Ronat, D. Yaffe, G. Yekutieli, I. Hammerman and J. Goldberg, *Nucl. Phys.* B80 (1974) 189.
8. G. Yekutieli, D. Yaffe, A. Shapira, E.E. Ronat, L. Lyons, U. Karshon, Y. Eisenberg, *Phys. Letters* 34B (1971) 101.
W. Gage, E. Colton, W. Chinowsky, *Nucl. Phys.* B46 (1972) 21.
G. Yekutieli, D. Yaffe, A. Shapira, E.E. Ronat, U. Karshon, Y. Eisenberg, *Nucl. Phys.* B40 (1972) 77.
W. Burdett, J. Hanlon, R.S. Panvini, E.O. Salant, W.H. Sims, J. Waters, M.S. Webster, R.R. Kinsey, T.W. Morris, *Nucl. Phys.* B48 (1972) 13.
J. Hanlon, R. Panvini, J. Waters and M. Webster, *Phys. Rev.* D12 (1975) 673.
9. J.D. Jackson, *Nuovo Cimento*, 34 (1964) 1644.
10. H.C. Dehne, E. Lohrmann, E. Raubold, P. Söding, M.W. Teucher, G. Wolf, *Phys. Rev.* 136B (1964) 843.
V. Alles-Borelli, B. French, Å. Frisk, L. Michejda, *Nuovo Cimento* 48A (1967) 360.
T. Ferbel, J.A. Johnson, H.L. Kraybill, J. Sandweiss, H.D. Taft, *Phys. Rev.* 173 (1968) 1307.
I. Borecka, G. Drews, W. Lenkeit, G. Comai, R. Santangelo, L. Bertanza, A. Bigi, R. Casali, P. Lariccia, R. Pazzi, R. Medves, C. Petri, *Nuovo Cimento*, 5A (1971) 19.
Ch. Walck, R. Carlsson, G. Ekspong, S.O. Holmgren, S. Nilsson, R. Stenbacka, P. Gregory, P. Mason, H. Muirhead and G. Warren, *Nucl. Phys.* B100 (1975) 61-73.
11. H. Bøggild, J. Eades, K. Hansen, H. Johnstad, R. Møllerud, L. Veje, P. Laurikainen, P. Lindblom, J. Tuominiemi, T. Jacobsen, S.O. Sørensen, Ø. Thingvold, G. Ekspong, I. Granström, S.O. Holmgren, S. Nilsson, T. Olhede, U. Svedin, N. Yamdagni, "Proton-proton reactions at 19 GeV/c with production of two and three pions", submitted to the XIVth International Conference on High Energy Physics, Vienna 1968.

- G. Yekutieli, S. Toaff, A. Shapira, E.E. Ronat, I. Lyons, Y. Eisenberg, Z. Carmel, A. Friedman, G. Maurer, R. Strub, C. Voltolini, P. Cuer, J. Grunhaus, Nucl. Phys. B18 (1970) 301.
- G. Alexander, O. Benary, G. Czapek, B. Haber, N. Kidron, B. Reuter, A. Shapira, E. Simopoulou, G. Yekutieli, Phys. Rev. 154 (1967) 1284.
- C. Caso, F. Conte, G. Tomasini, L. Casè, L. Mosca, S. Ratti, I. Tallone-Lombardi, I. Bloodworth, I. Lyons, A. Norton, Nuovo Cimento 55 (1968) 66.
- G. Kayas, J. Le Guyader, M. Sene, T.P. Yiou, J. Alitti, Nguyen Thuc Diem, S. Smadja, J. Ginestet, D. Manesse, Tran Ha Ahn, Nucl. Phys. B5 (1968) 169.
- W.E. Ellis, T. Morris, R.S. Panvini, A.M. Thorndike, "A description of final states with three-, four-, and five-particles in pp interactions at 28.5 GeV/c", Paper submitted to the Lund International Conference on Elementary Particles, Lund 1969.
12. a) H.O. Cohn, R.D. McCulloch, W.M. Bugg, G.T. Condo, Nucl. Phys. B21 (1970) 505, Phys. Letters 26B (1968) 9.
- b) A.R. Kirschbaum, E. Colton, Phys. Rev. 7D (1973) 1324.
- c) A. Shapira, G. Yekutieli, D. Yaffe, S. Toaff, E.E. Ronat, I. Lyons, U. Karshon, B. Haber, Y. Eisenberg, Nucl. Phys. B23 (1970) 583.

FIGURE CAPTIONS

- Fig. 1 Various distributions illustrating the separation of the coherent channel $pd \rightarrow pd \pi^+ \pi^-$ from the non-coherent reaction $pd \rightarrow ppn \pi^+ \pi^-$. The full distributions represent all events fitting the non-coherent reaction and the shaded areas correspond to events with an additional coherent interpretation.
- Fig. 2 The t_{dd}' distribution for the channel $pd \rightarrow pd \pi^+ \pi^-$. The straight lines are fits to singel exponentials.
- Fig. 3 The t_{dd}' distribution for the channel $pd \rightarrow pd \pi^+ \pi^-$. The straight lines are fits to singel exponentials.
- Fig. 4 The t_{dd}' distribution for the channel $pd \rightarrow nd \pi^+ \pi^+ \pi^-$. The straight line is a fit to a singel exponential.
- Fig. 5 The angular distribution in the laboratory frame of the spectator for the reaction $pd \rightarrow p_s pp \pi^-$. The line is the prediction of the invariant flux factor.
- Fig. 6 Scatterplot of $p_{lab}(p_s)$ versus p_{lab} (neutron) for the slow neutrons in the reaction $pd \rightarrow ppn \pi^+ \pi^-$, where p_s is the proton with the smallest laboratory momentum. The diagonal line identifies the spectator nucleon. The histograms b) and c) show the spectator momentum distributions of the proton spectator and neutron spectator respectively. The shaded area represents the 3-prong events.
- Fig. 7 Cross sections for the reactions $pn \rightarrow pp \pi^-$, $pn \rightarrow pp \pi^- \pi^0$, $pn \rightarrow pn \pi^+ \pi^-$ and $pd \rightarrow pd \pi^+ \pi^-$ as function of the beam momentum p_{lab} . The 28 GeV/c cross section is commented in the text.
- Fig. 8 The $M(N\pi)$ distributions for the $p_F n_B \pi^+ \pi^-$ channel.
- Fig. 9 Scatter plot of $M(p_F \pi^+)$ versus $M(n_B \pi^-)$ for the $p_F n_B \pi^+ \pi^-$ channel.
- Fig. 10 The cross sections for associated $\Delta\Delta$ production as function of the beam momentum p_{lab} for the reactions $\bar{p}p \rightarrow \bar{\Delta}^{++} \Delta^{++}$, $pp \rightarrow \Delta^{++} \Delta^0$ and $pn \rightarrow \Delta^{++} \Delta^-$. The line shown is of the form p_{lab}^{-n} with $n = 2.5$.
- Fig. 11 The $M(N\pi)$ distributions for the $n_F p_B \pi^+ \pi^-$ channel.

- Fig. 12 The $M(N\pi)$ distributions for the $pp\pi^-\pi^0$ channel.
- Fig. 13 The $M(p_F\pi^+\pi^-)$ and $M(n_B\pi^+\pi^-)$ mass distributions for the $p_F n_B \pi^+\pi^-$ channel. The shaded regions show the distribution when the smallest of the two possible $N\pi^+\pi^-$ combinations is chosen.
- Fig. 14 The $M(N\pi^+\pi^-)$ distribution for the $p_F n_B \pi^+\pi^-$ channel.
- Fig. 15 The $M(p_B\pi^+\pi^-)$ and $M(n_F\pi^+\pi^-)$ mass distributions for the $p_B n_F \pi^+\pi^-$ channel.
- Fig. 16 The $M(p_F\pi^-\pi^0)$ and $M(p_B\pi^-\pi^0)$ mass distributions for the $pp\pi^-\pi^0$ channel.
- Fig. 17 The $M(\pi^+\pi^-)$ and $M(\pi^-\pi^0)$ mass distribution for the $pn\pi^+\pi^-$ and $pp\pi^-\pi^0$ channels.

TABLE 1. Fits to $t' = |t - t_{\min}|$ distributions for the coherent channels

Final state	Region fitted	Slope	$\chi^2/\text{degrees of freedom}$
$p d \pi^+ \pi^-$, 3 and 4 prong	.00 - .15	28 ± 1	7.5/13
$p d \pi^+ \pi^-$, 4 prong	.03 - .15	30 ± 2	5.3/10
$p d \pi^+ \pi^-$, 4 prong, no d^*	.03 - .15	29 ± 2	6.7/10
$p d \pi^+ \pi^- \pi^0$, 4 prong	.01 - .12	20 ± 2	7.7/9
$p d \pi^+ \pi^- \pi^0$, 4 prong no d^*	.01 - .12	26 ± 1	11.2/9
$n d \pi^+ \pi^-$, 4 prong	.01 - .12	25 ± 3	9.3/9

TABLE 2. Channel cross sections. F and B denote forward and backward in the center of mass system

Channel	Events	σ (mb)
$pn \rightarrow pp\pi^-$	1209	0.64 ± 0.03
$pn \rightarrow pp\pi^-\pi^0$	1169	0.66 ± 0.08
$pn \rightarrow n \begin{matrix} p \\ F \\ B \end{matrix} \pi^+\pi^-$	1053	0.60 ± 0.07
$pn \rightarrow p \begin{matrix} n \\ F \\ B \end{matrix} \pi^+\pi^-$	3790	2.1 ± 0.2
$pd \rightarrow pd\pi^+\pi^-$	809	0.42 ± 0.03
no d^*	795	0.35 ± 0.03
$pd \rightarrow pd\pi^+\pi^-\pi^0$	779	0.36 ± 0.04
no d^*	510	0.26 ± 0.03
$pd \rightarrow nd\pi^+\pi^+\pi^-$	523	0.15 ± 0.02

TABLE 3.




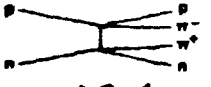








$p n \rightarrow p_f n_b \pi^+ \pi^-$	$p n \rightarrow p_b n_f \pi^+ \pi^-$	$p n \rightarrow p p \pi^+ \pi^-$
3790 EVENTS	1053 EVENTS	1169 EVENTS
 $\Delta Q = 1$ 34%	 $\Delta Q = 2$ 13%	 $\Delta Q = 0$ 29%
 $\Delta Q = 1$ 11%	 $\Delta Q = 0$ 37%	 $\Delta Q = 1$ 19%
 $\Delta Q = 0$ 25%	 $\Delta Q = 1$ 24%	 $\Delta Q = 1$ 19%
 $\Delta Q = 0$ 30%	 $\Delta Q = 0$ 26%	 $\Delta Q = 0$ 33%

TABLE 4. Cross sections for Δ production and results of fits to double exponentials $Ae^{-b_1 t} + Be^{-b_2 t}$

Channel	Cross section (mb)	b_1 (GeV/c) ⁻²	b_2 (GeV/c) ⁻²	B/A
$pn \rightarrow \Delta_F^{++} n \pi^-$	0.72 ± 0.09	25 ± 7	4 ± 1	0.36 ± 0.11
$pn \rightarrow p \pi^+ \Delta_B^-$	0.74 ± 0.09	18 ± 5	3 ± 1	0.19 ± 0.11
$pn \rightarrow \Delta_F^{++} \Delta_B^-$	0.14 ± 0.03	19 ± 2	-	-

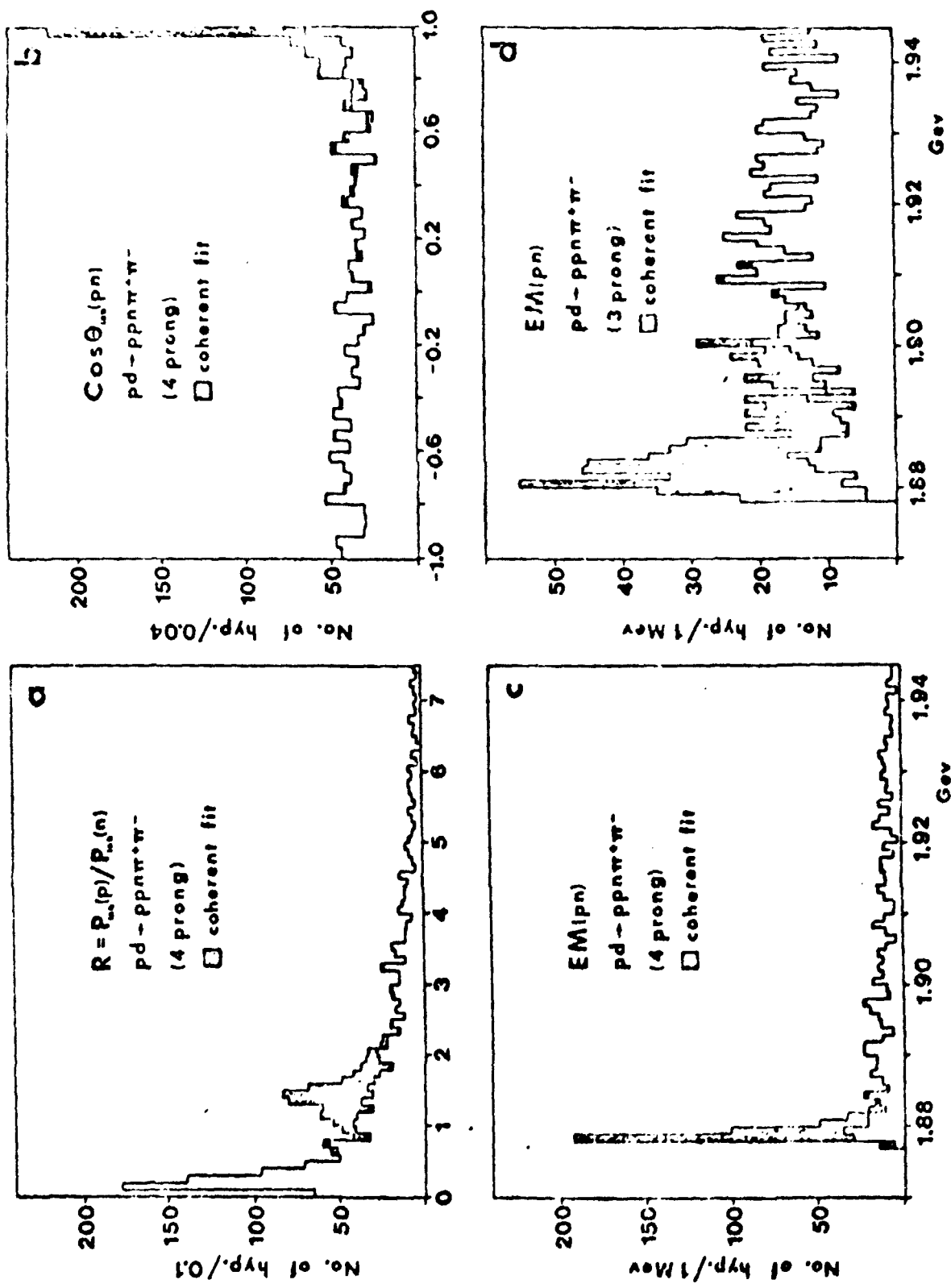


Fig 1

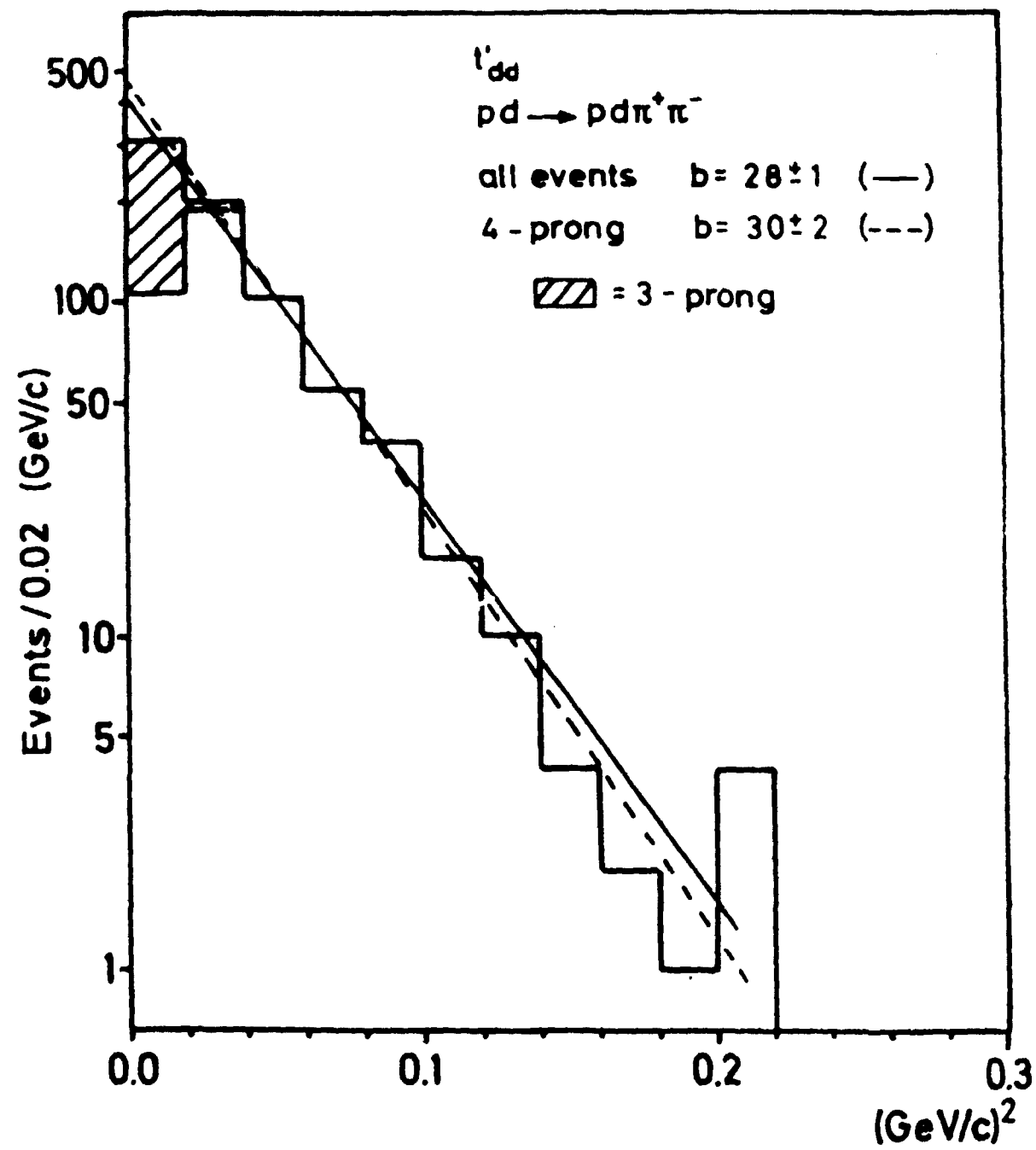


Fig 2

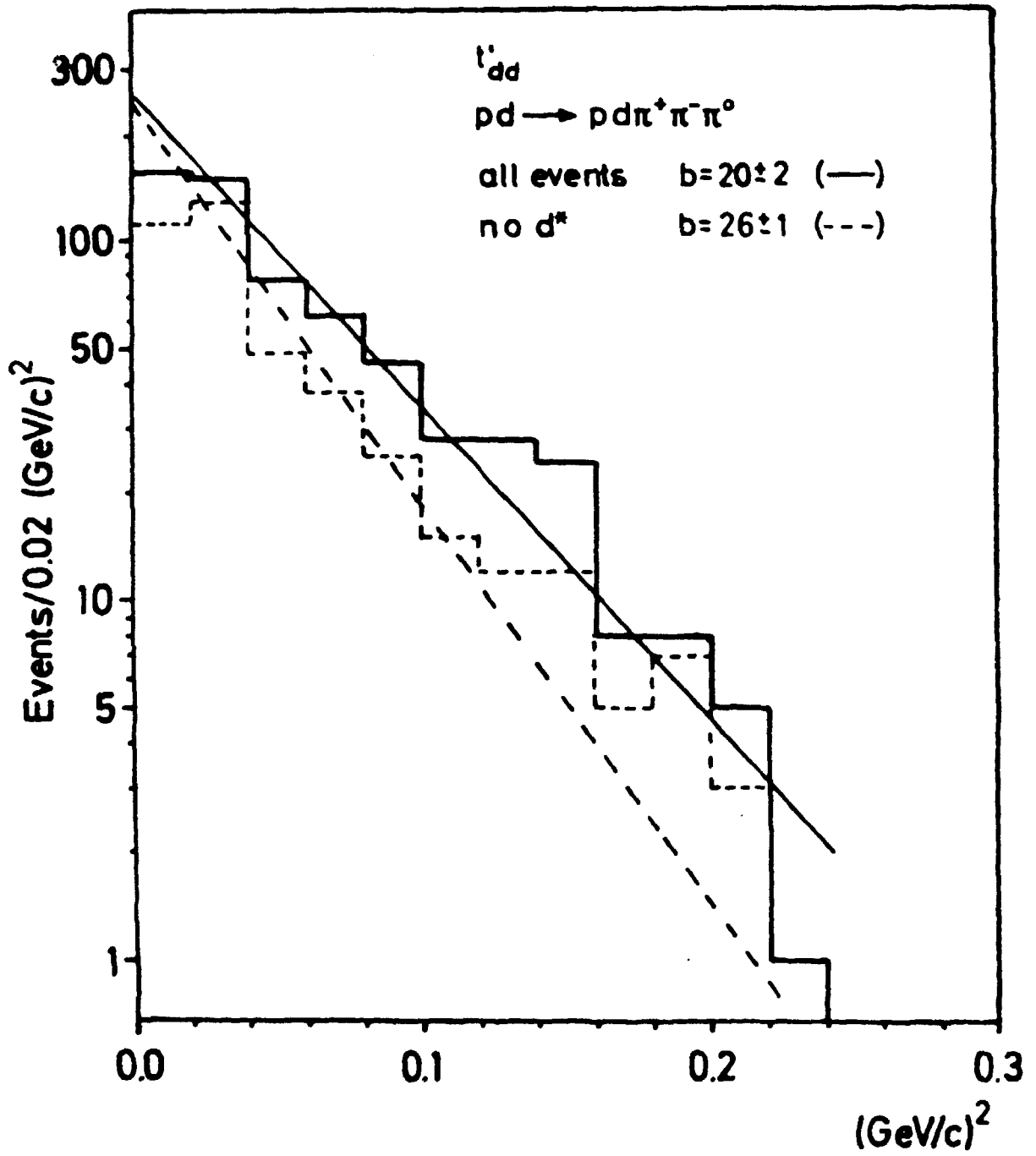


Fig 3

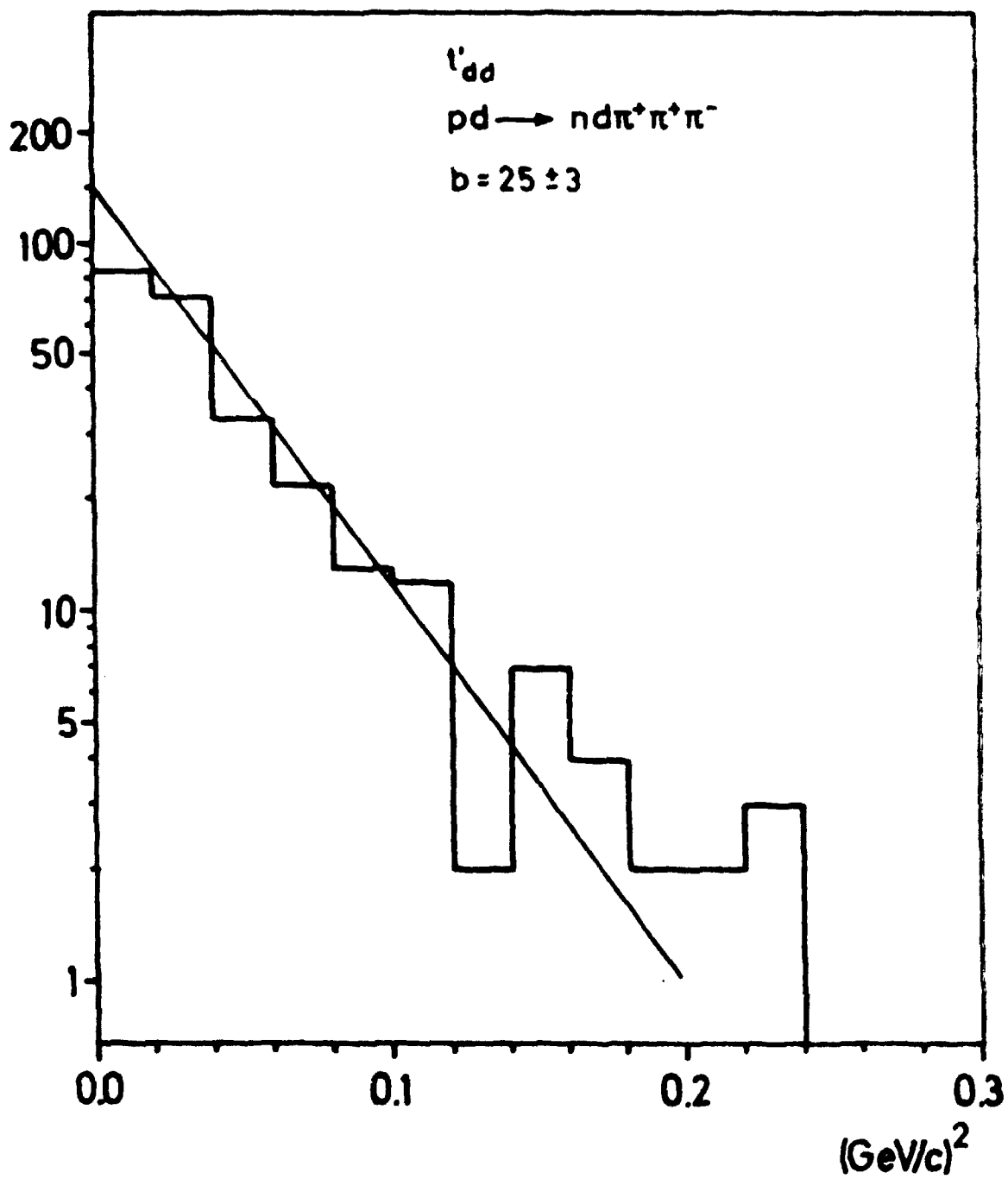


Fig 4

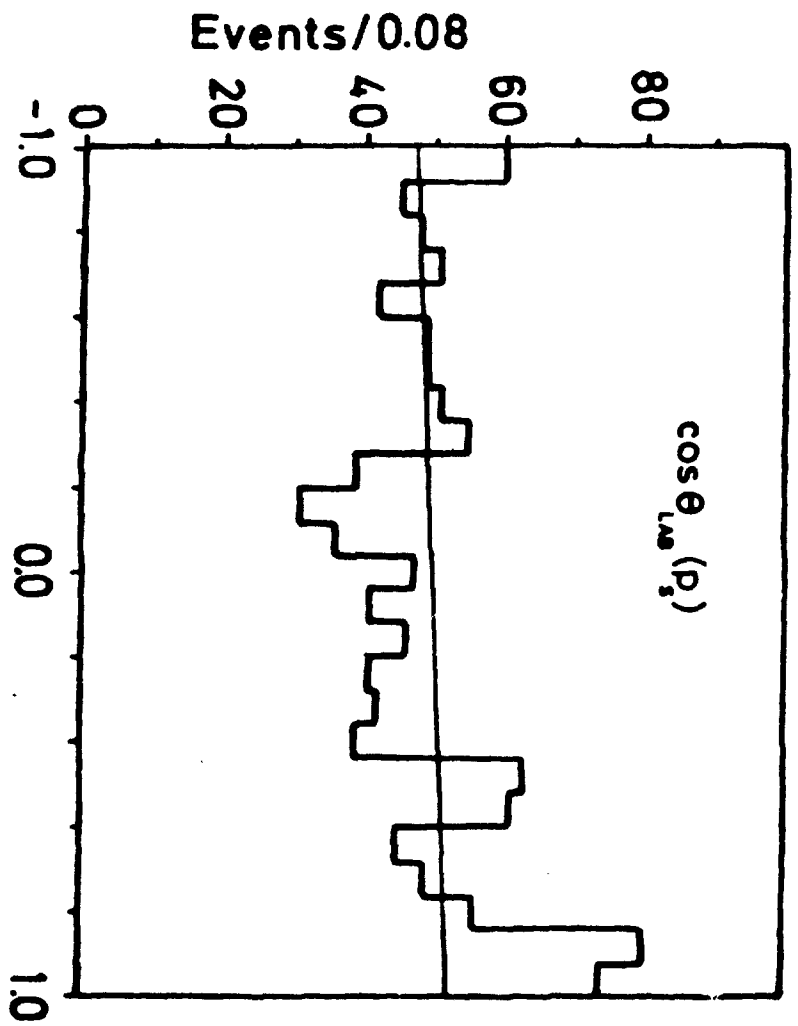


Fig 5

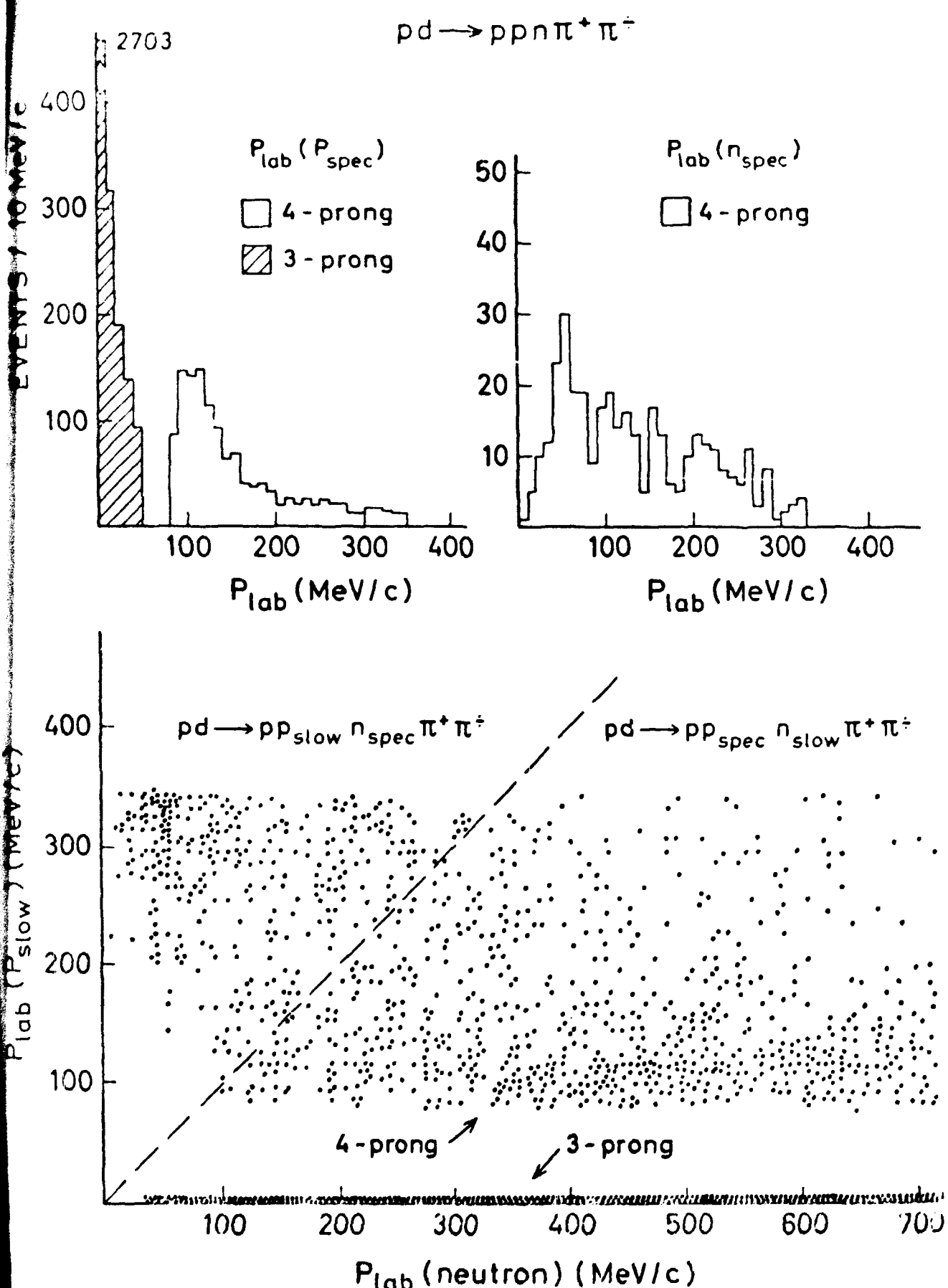


Fig 6

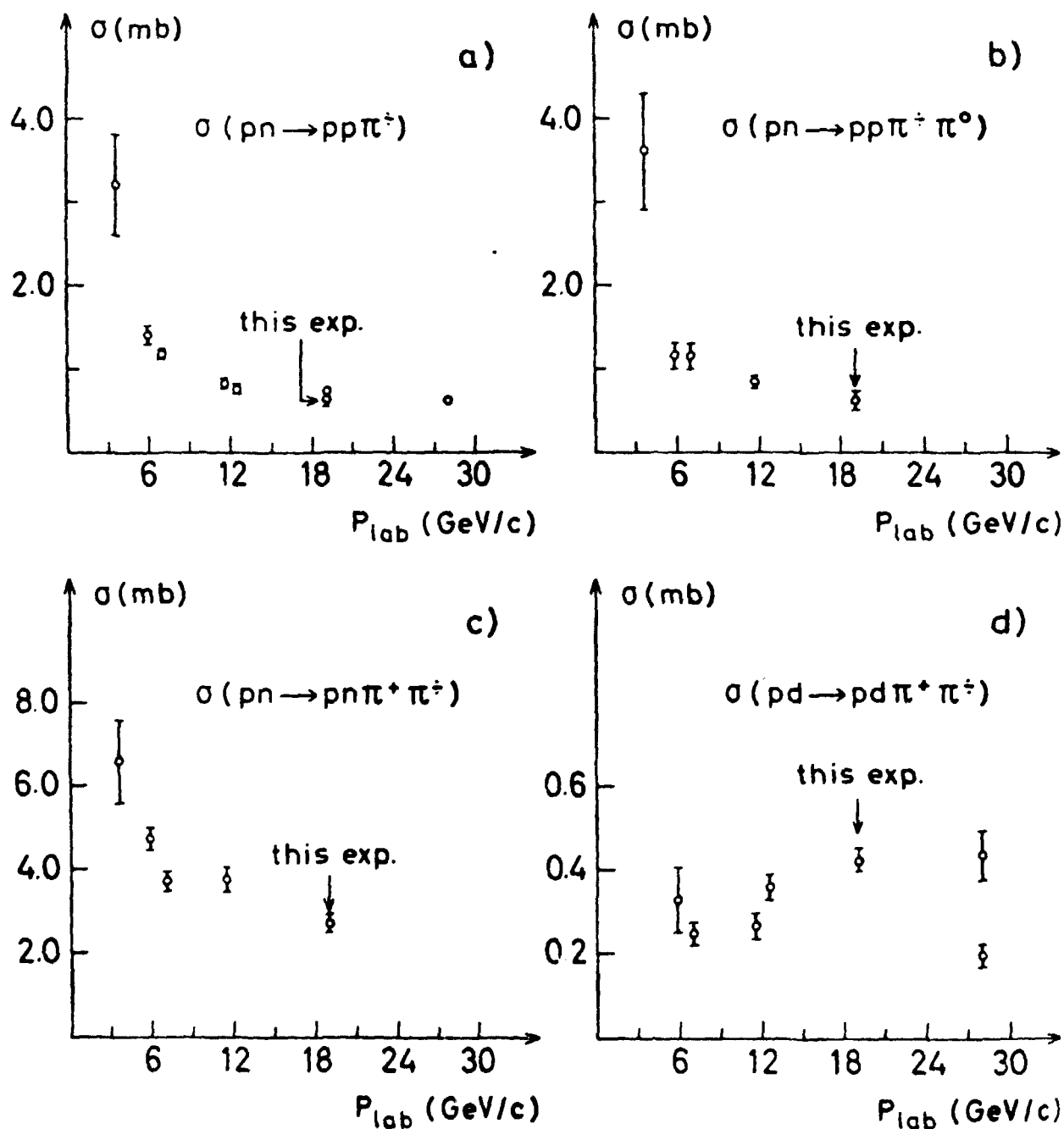


Fig 7

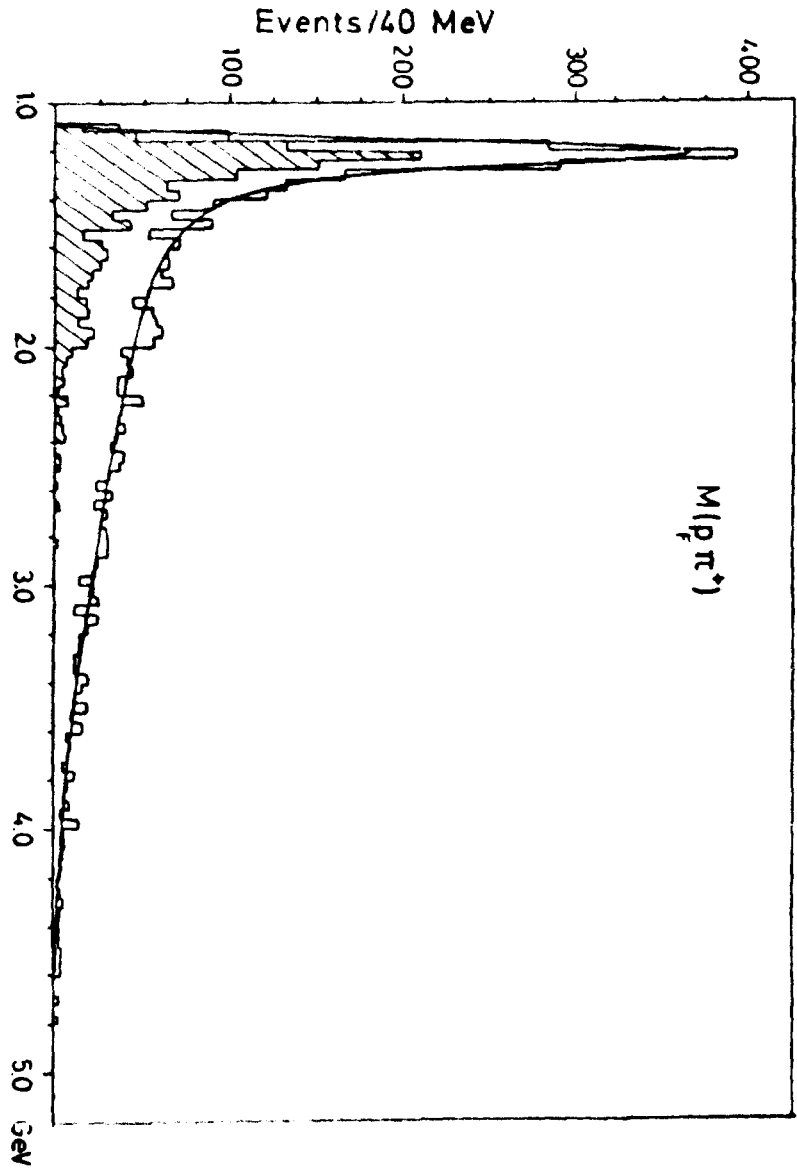
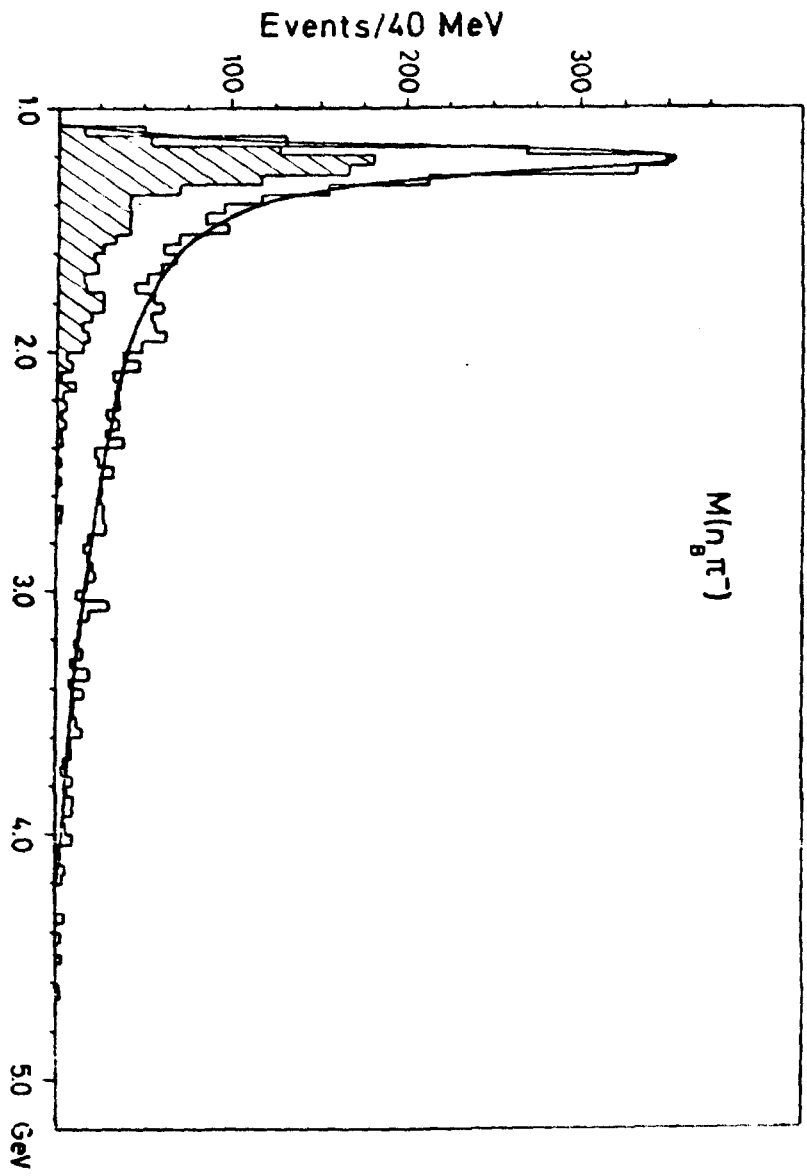


FIG 8 a

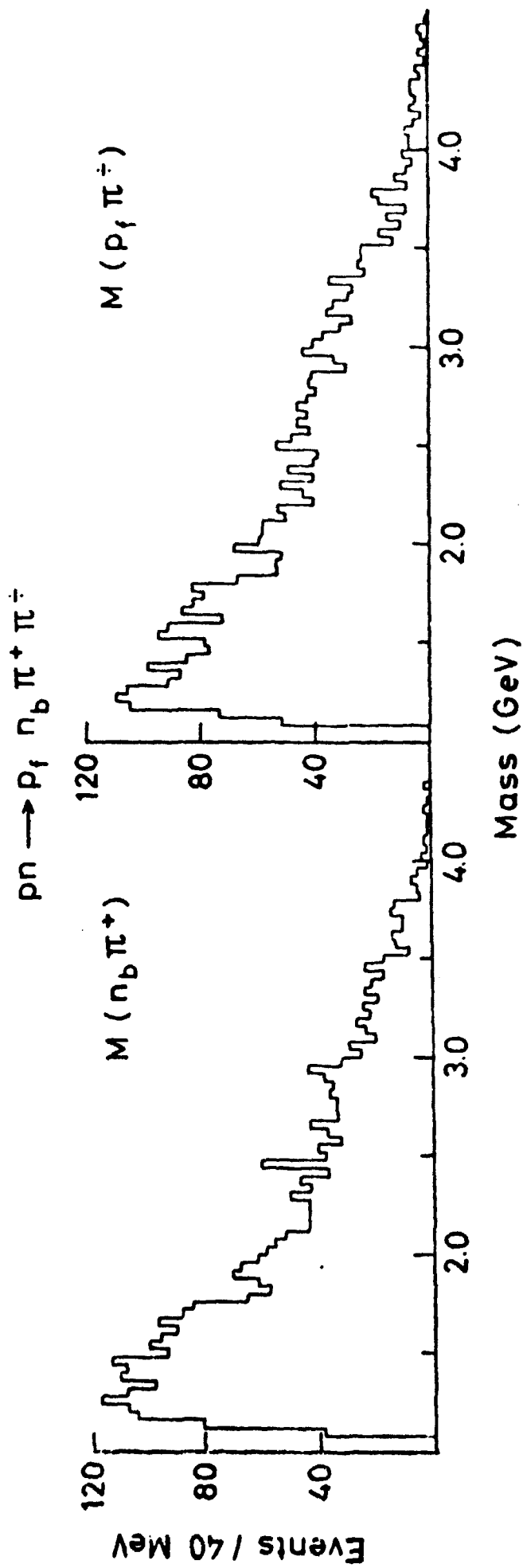


Fig 8 b

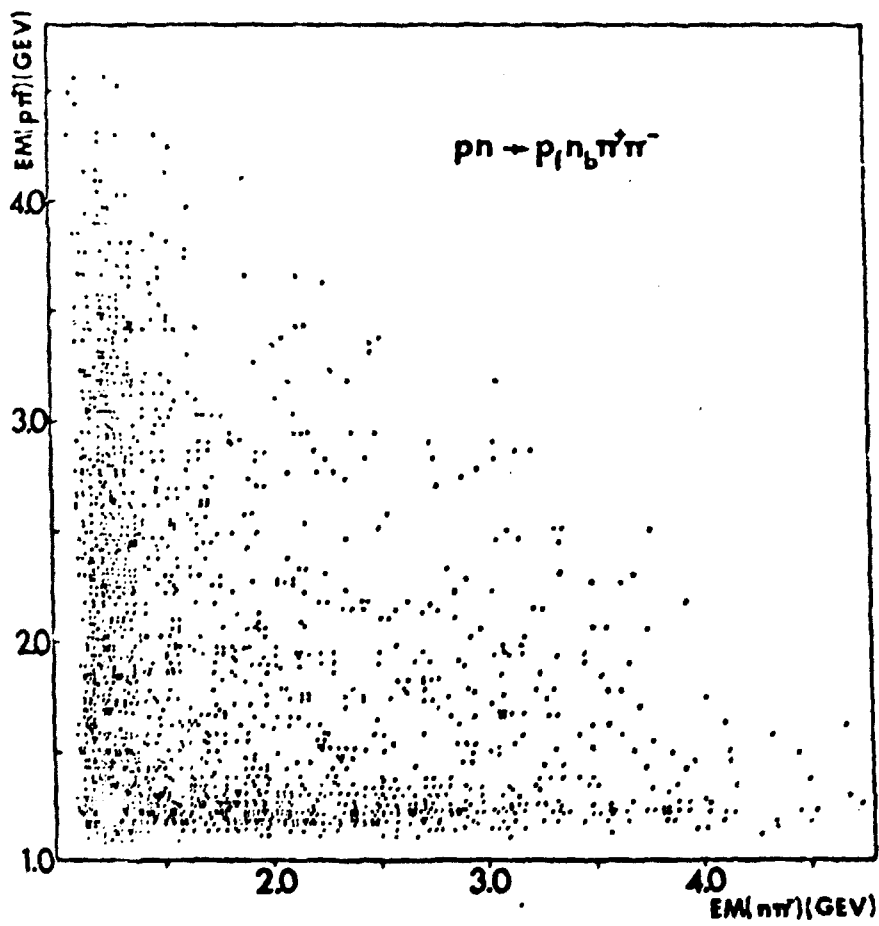


Fig 9

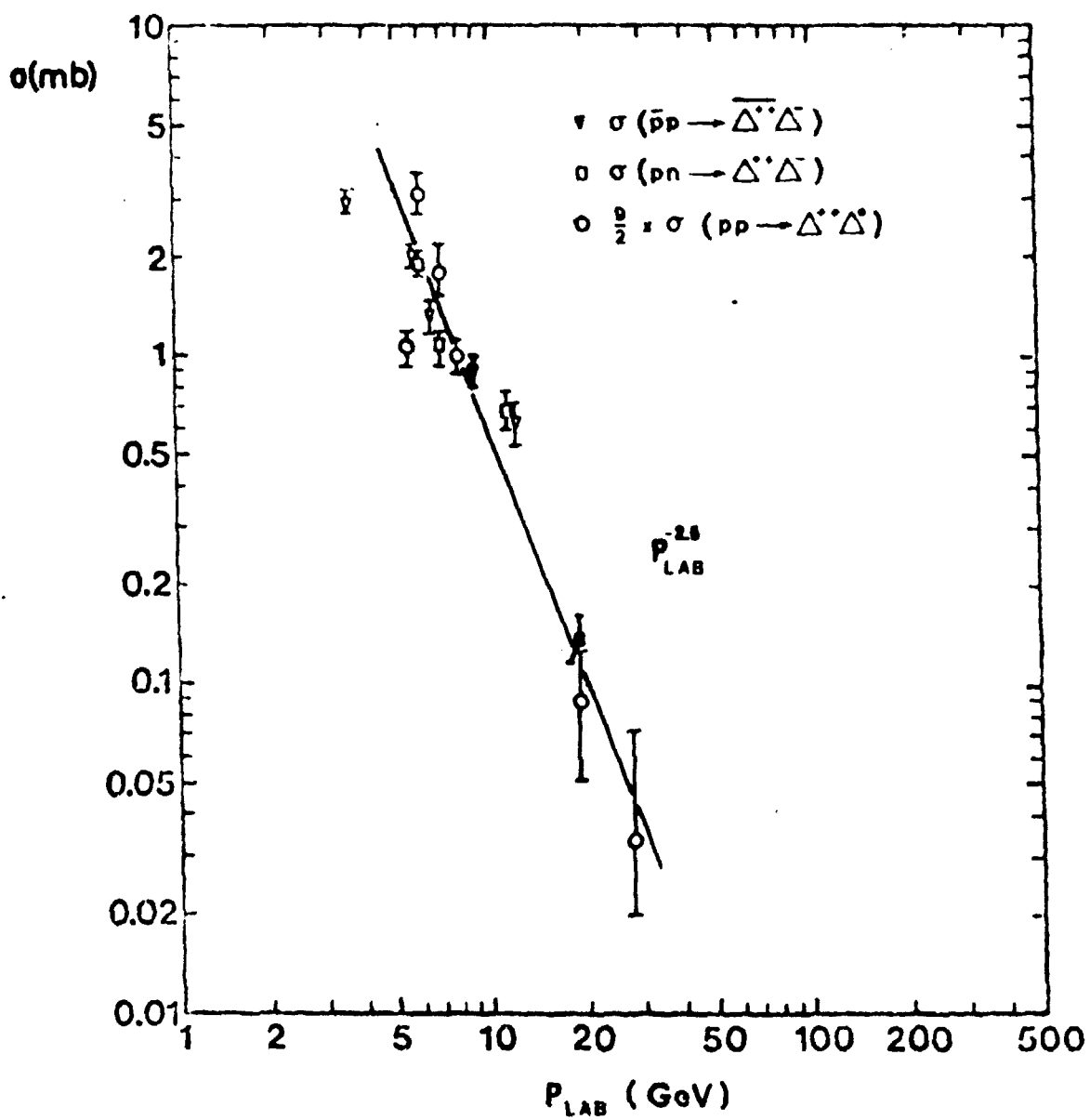


Fig 10

$p\bar{n} \rightarrow p_b n_f \pi^+ \pi^-$

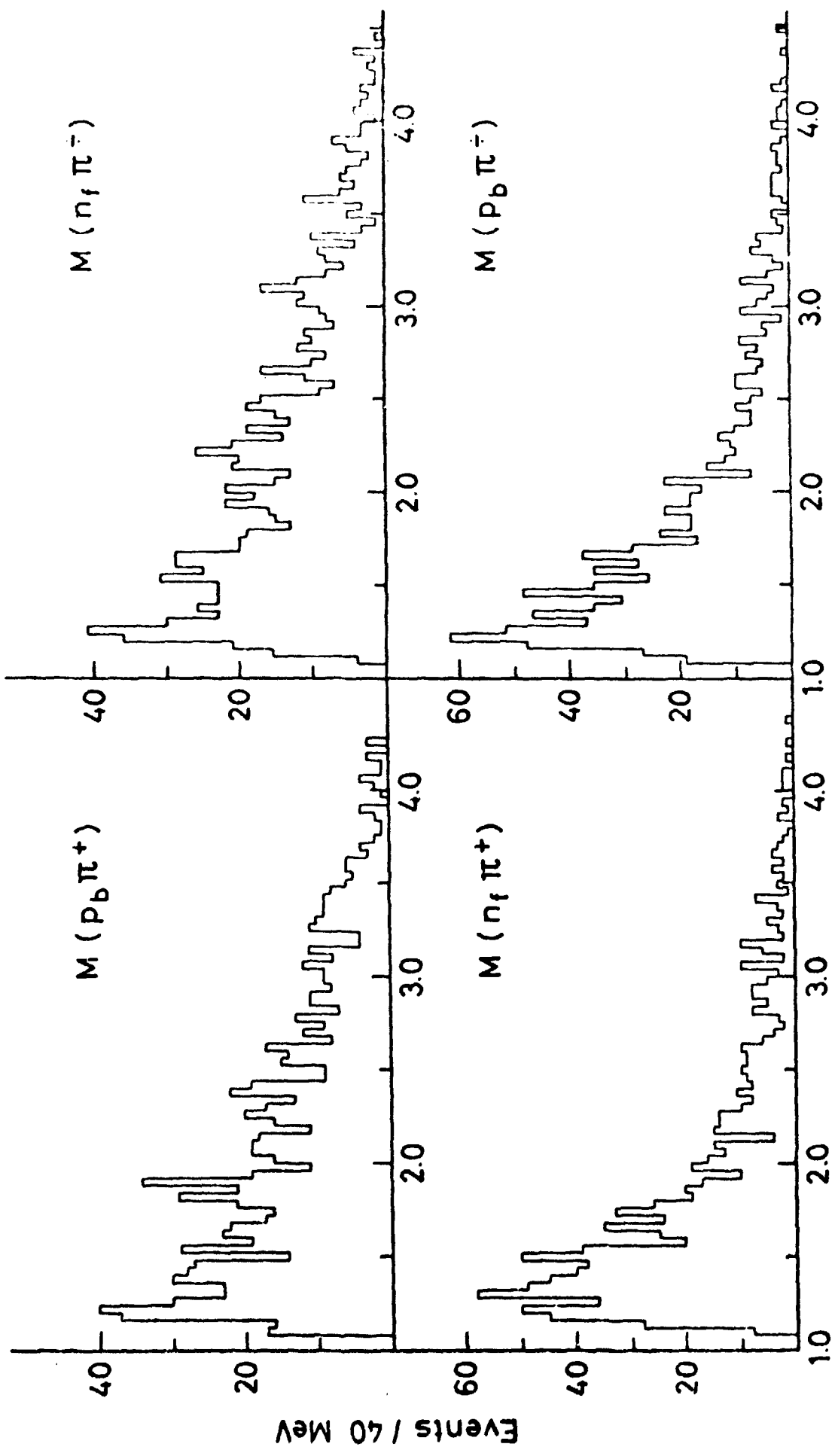


Fig 11

$p\bar{n} \rightarrow p_f p_b \pi^+ \pi^-$

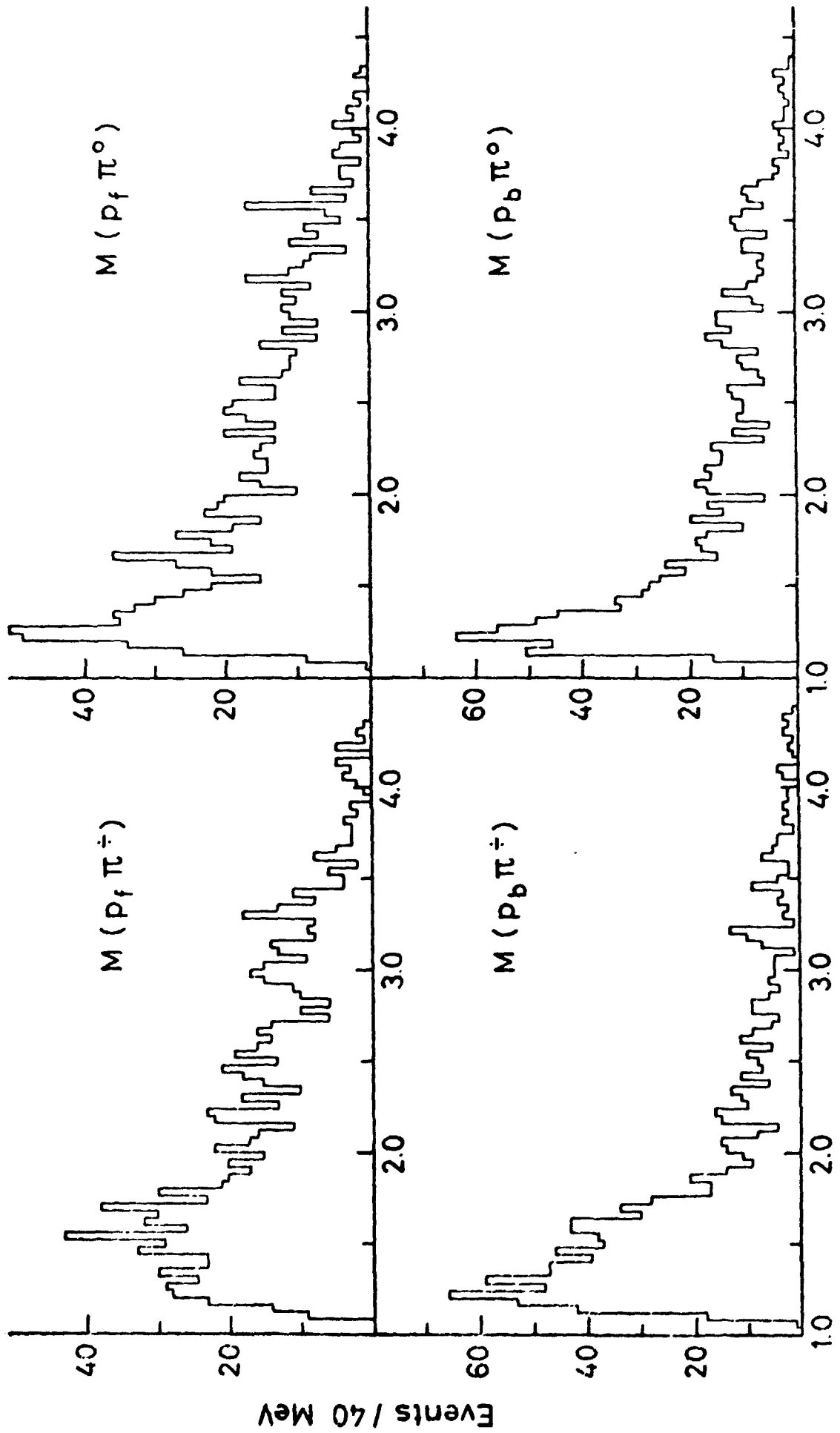
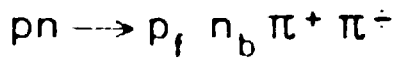


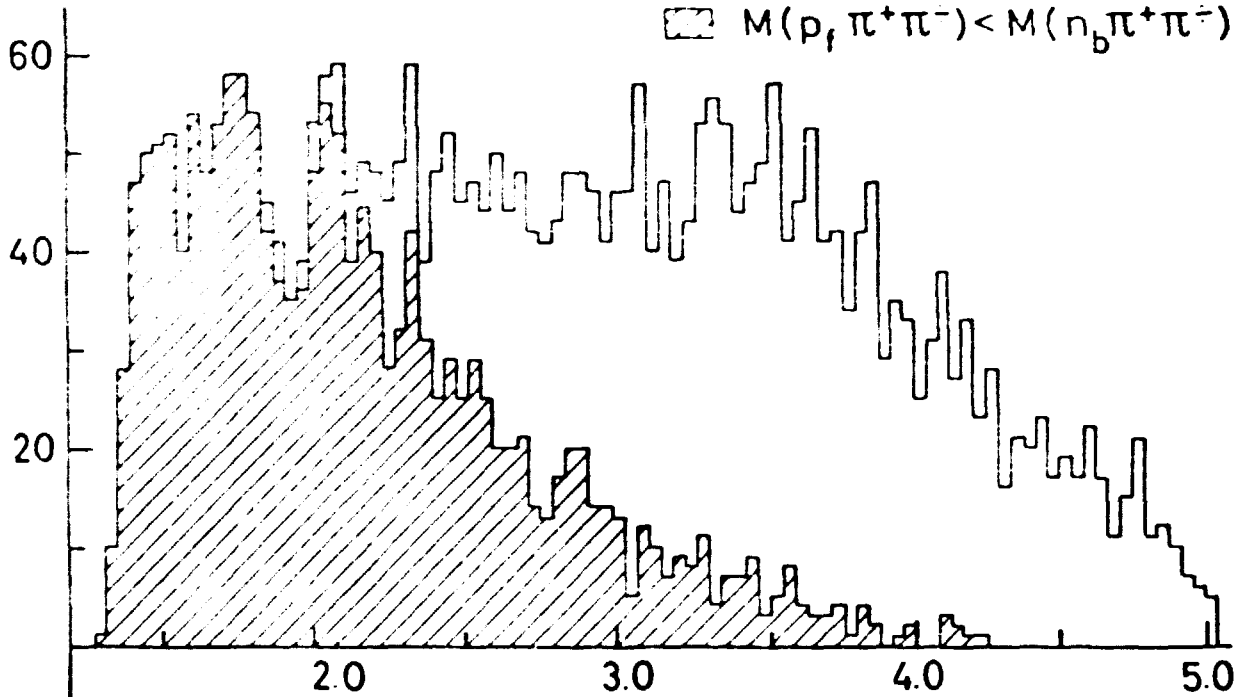
FIG. 12



$$M(p_f \pi^+ \pi^-)$$

□ All events

▨ $M(p_f \pi^+ \pi^-) < M(n_b \pi^+ \pi^-)$



$$M(n_b \pi^+ \pi^-)$$

□ All events

▨ $M(n_b \pi^+ \pi^-) < M(p_f \pi^+ \pi^-)$

Events / 40 MeV

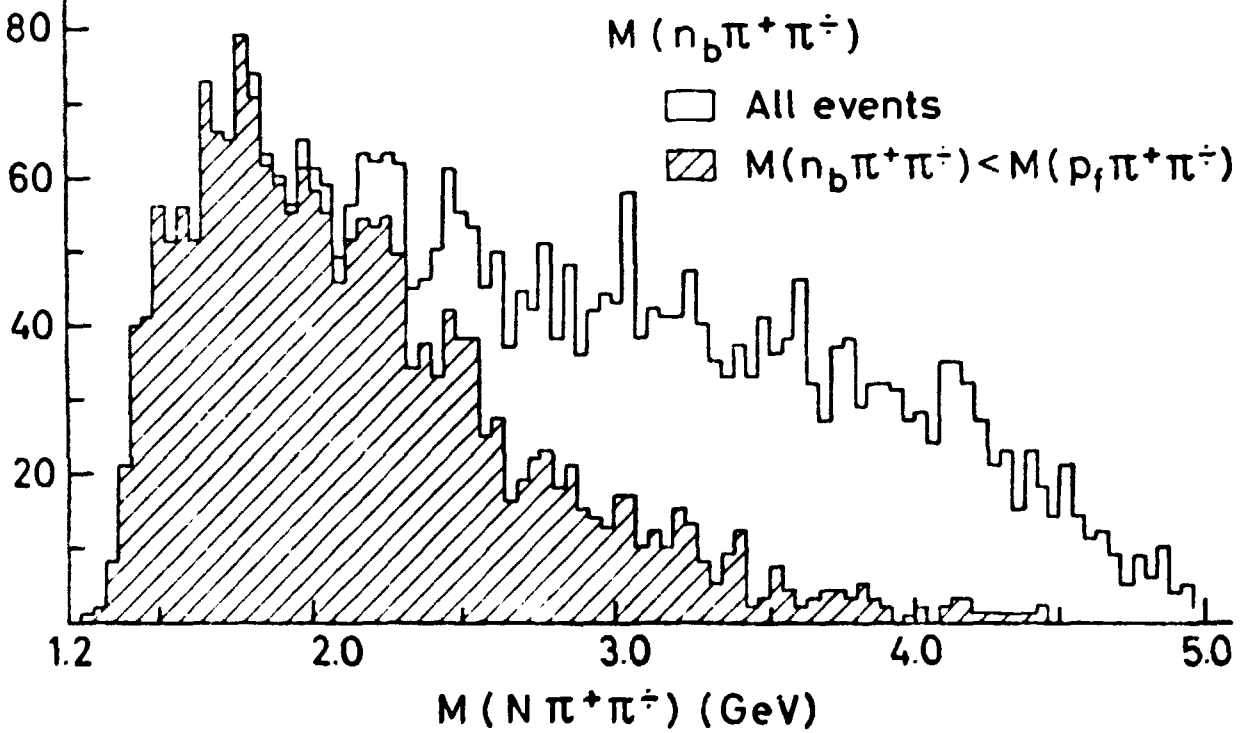


Fig 13

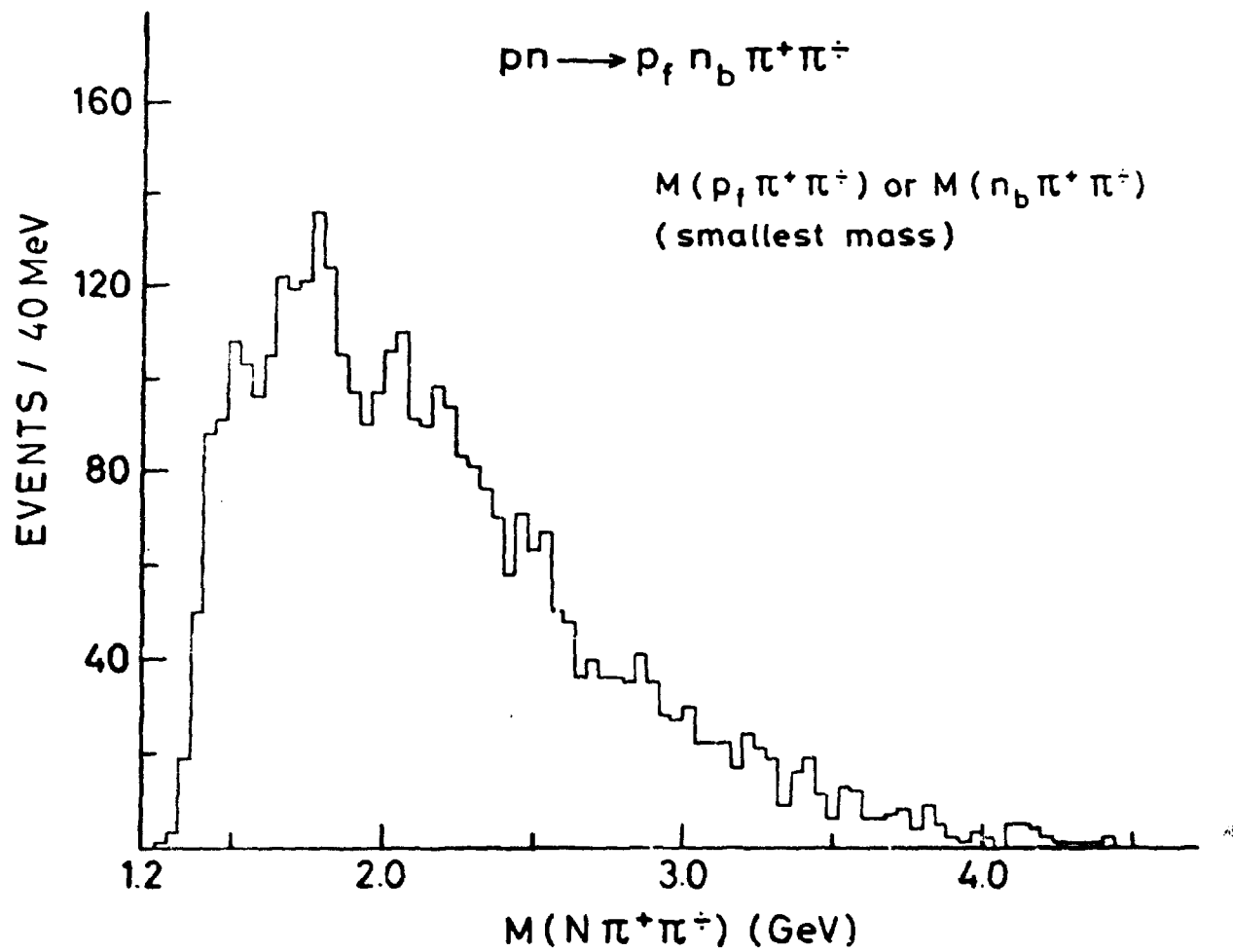


Fig 14

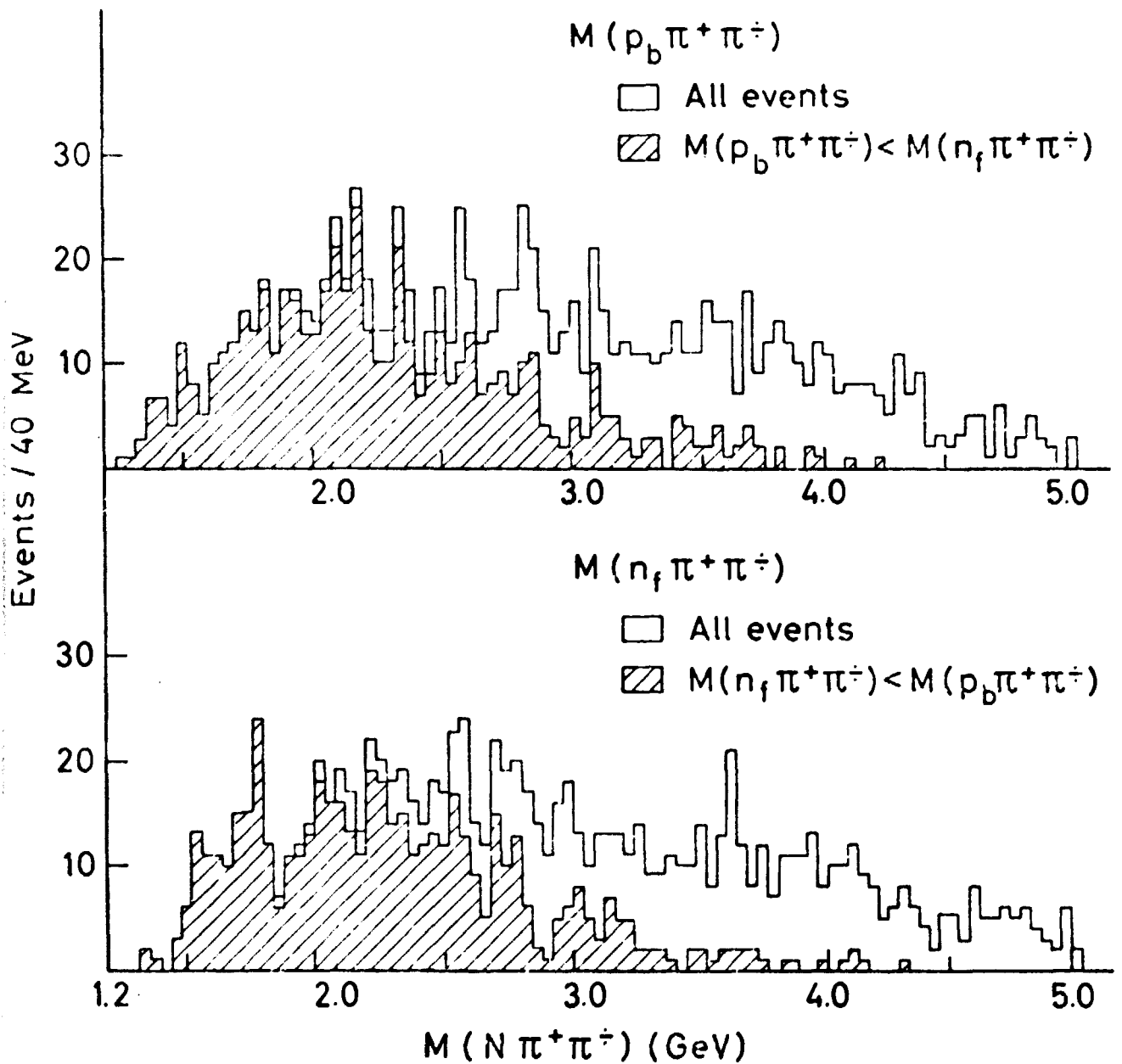


Fig 15

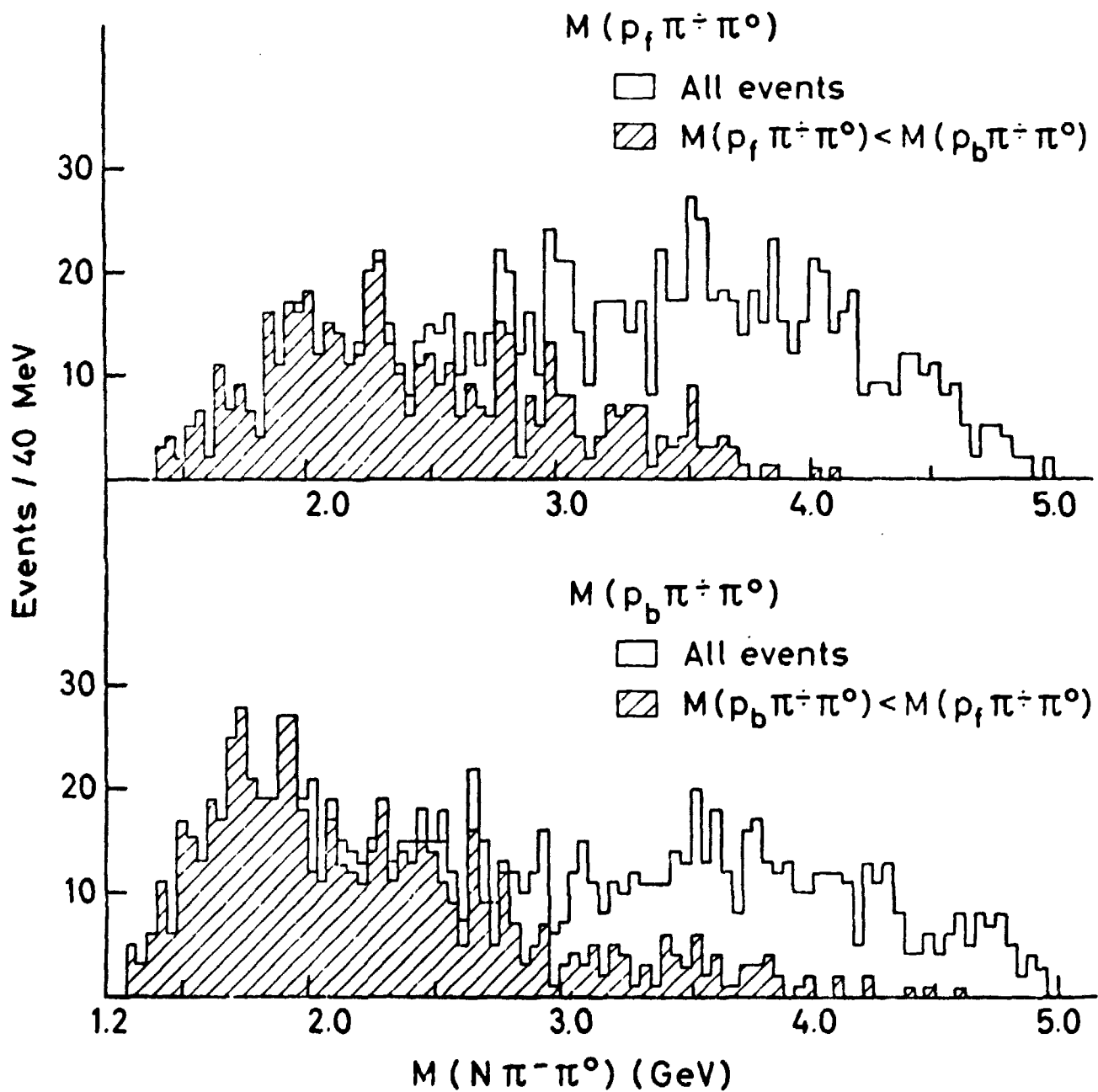
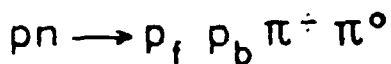


Fig 16

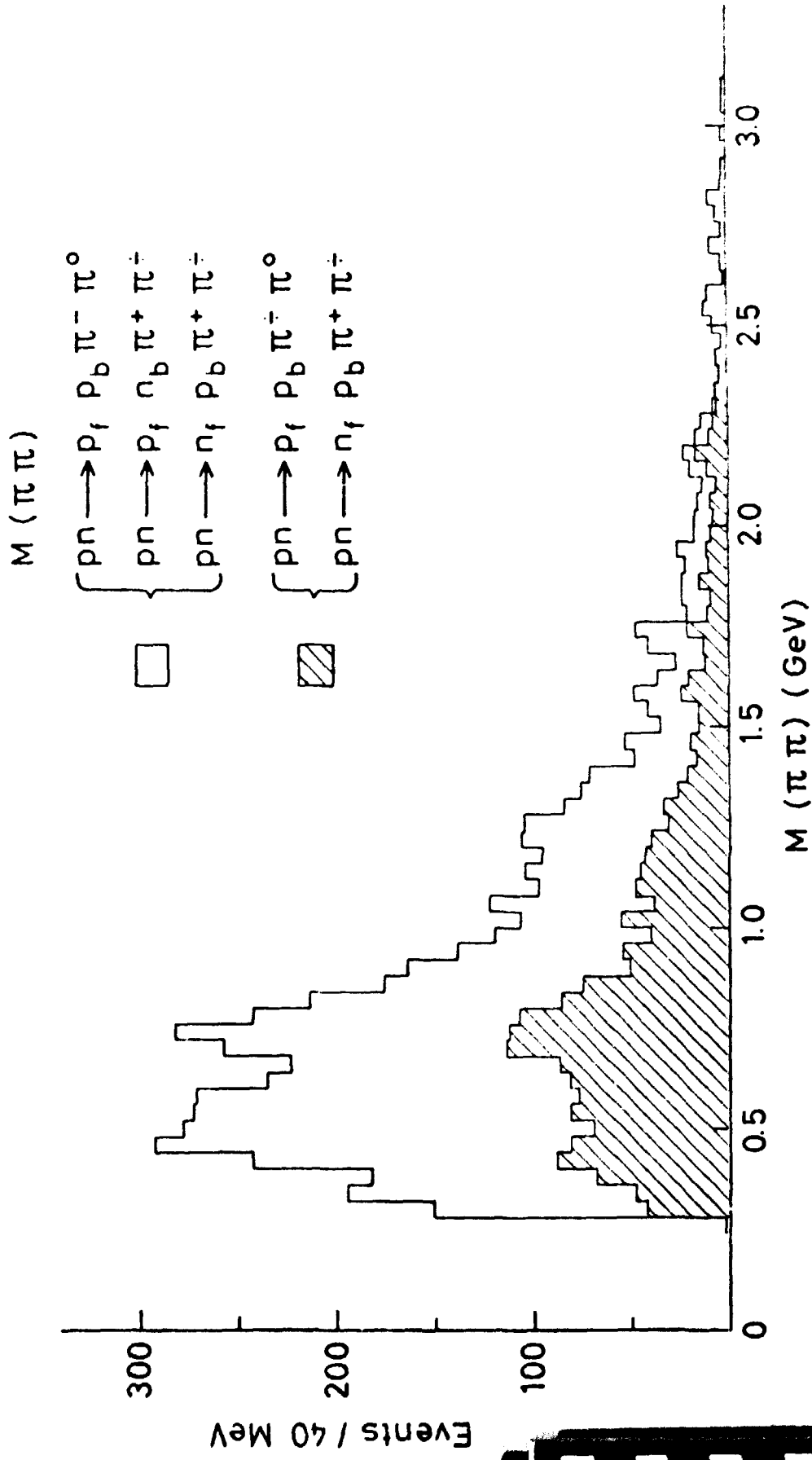


FIG 17

UNIVERSITY OF STOCKHOLM
INSTITUTE OF PHYSICS
VANADISVÄGEN 9
S-113 46 STOCKHOLM
SWEDEN